Model Predictive Torque Control of a Switched Reluctance Drive with Heat Dissipation Balancing in a Power Converter

Alecksey Anuchin, Valentina Podzorova
Department of Electric Drives
Moscow Power Engineering Institute
Moscow, Russia
anuchin.alecksey@gmail.com

Viktoriya Popova, Igor Gulyaev
Electronics and Nanoelectronics Department
Ogarev Mordova State University
Saransk, Russia

Fernando Briz
Department of Electrical, Electronic, Computers and Systems Engineering
University of Oviedo
Gijón, Spain

Yuriy Vagapov
Electrical Engineering Division of Engineering, Computing and Applied Physics
Wrexham Glyndwr University
Wrexham, United Kingdom

***Abstract*—The switched reluctance machines are known for their torque pulsations. The precise torque control is usually implemented by varying commutation angles and applying direct torque control. But still the problem of pulsation occurs during phase change. This paper proposes a model predictive direct torque control method, which cost function takes into account both torque and current control including heat dissipation balancing in a power converter. The proposed control strategy was examined using a simulation model and provides precise torque control. Heat dissipation balancing helps to equalize power modules temperature increasing the maximum output power of the power converter.**

Keywords—switched reluctance drive; model predictive control; direct torque control; active thermal control.

I. INTRODUCTION

Switched reluctance motor drives (SRD) attract attention in the academic research over past three decades, when commercial IGBTs appeared on the market [1]. It was said that SRD will become industrial standard for the drive, but still we have very few applications of these electrical machines. The main problems of SRD remain the same for many years, and they are: high torque pulsations over entire speed range [2], [3], big radial forces and expensive power electronics converter [4].

The power converter contains asymmetrical bridges, which utilize the same amount of silicon, whereas the production volume of such devices is much smaller resulting in higher price per kW of the output power. The problem can be partially solved in the multi-phase machines, where the full-bridge topology can be utilized, but this brings restrictions to the commutation pattern limiting the controllability of the drive. High radial forces occur due to the misalignment of stator and rotor, which can be reduced if smaller tolerances are used when manufacturing. While the manufacturing of the SRD seems to be simple, the precise lamination, shaft, bearings and encloser manufacturing makes this machine more expensive than conventional induction motor.

The torque pulsations can be partially reduced by means of proper control strategy [5]. Forming the right current shapes in the phases of the machine it is possible to obtain constant output torque [6]. But still the correct current shape cannot be realized over the entire speed range due to the voltage constrains.

Many authors consider the open-loop operation of the SRD optimizing the commutation angles of the power-electronics converter [5]. While simple this approach needs precalculation of angle of advance and cut-off angle for the particular electrical machine as a function of the current speed. This approach cannot guaranty high stability of the torque, but it is simple enough to be implemented using low-cost microcontrollers. More sophisticated solution is the direct torque control for SRD [7] [8], which uses the torque maps of the motor with respect to the current, but still it has problems while operating at voltage constrains [9] and when the conducting phase changes [10]. The model predictive control systems can provide maximum utilization of the inverter together with the precise torque stabilization [11]. In this paper model predictive control strategy is considered, which takes into account the temperatures of the power modules of the power converter. The equalization of the modules' temperatures due to heat dissipation balancing helps to increase output power of the power electronics converter.

The research was performed with the support of the Russian Science Foundation grant (project 15-19-20057).

II. ELECTROTHERMAL MODEL OF SRD

A. Electrical model of SRD

The most popular configuration of the three-phase SRD has 6/4 topology (see Fig. 1) with six teeth stator and four teeth rotor [1]. Each stator tooth has its coil. Two opposite coils, connected serially or in parallel, form the stator phase winding. Each phase is fed from its own asymmetrical bridge inverter which forms an unipolar current in it. The typical operation cycle for a single phase starts in the position with the smallest inductance (curve *A* in Fig. 2a).

The current control in the windings of switched reluctance motor (SRM) is usually performed using hysteresis current controllers. There are three modes of operation:

- both switches are on, and the full DC-link voltage is applied to the motor winding (see Fig. 3a);
- one switch is on and another is off, and the phase is short-circuited with zero voltage applied (see Fig. 3b and c);
- both switches are off, and the negative DC-link voltage is applied to the winding through freewheeling diodes, while current continue flowing in the winding (see Fig. 3d).

During the rotor rotation the phase inductance changes till it reaches its maximum value (curve *B* in Fig. 2a). In this point the phase should be switched off. The mechanical work is equal to the area "*oabo*".

For the simplification of the equations of the model, the relationship between the flux linkage and the current was linearized (see Fig. 2b) [12]. It was assumed that the phase inductance changes according to the following equation:

$$L = L_{av} - \Delta L \cos\theta, \tag{1}$$

where L_{av} is the average inductance, ΔL is the half difference between maximum and minimum inductances, and θ is the rotor electrical angular position.

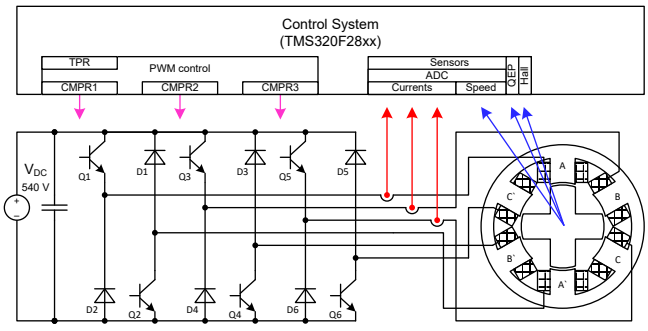

Fig. 1. SRD configuration.

The switched reluctance machines are designed to work in saturation. This gives better efficiency and better power factor [1]. The saturation current in the model is the same for any rotor position. If the phase current reaches the saturation current level the differential inductance becomes equal to the minimal phase inductance as it is shown in Fig. 2b. This is relatively rude approximation, but it is acceptable for the purpose of this model.

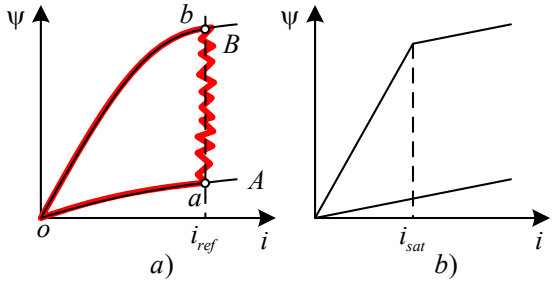

Fig. 2. Relationship between flux linkage and current (a—for a real motor; b—for the linearized motor model).

Fig. 3. Operation modes of a single phase of SRD.

The flux linkage of each phase, which are assumed to be magnetically independent, can be evaluated by the following equation:

$$\frac{\mathrm{d}\psi}{\mathrm{d}t} = v - iR, \tag{2}$$

where v is the voltage applied, i is the phase current, and R is the active resistance of the winding. This equation is implemented using Euler integration method as:

$$\psi_k = \psi_{k-1} + (v - iR)h, \tag{3}$$

where ψ_k and ψ_{k-1} are the new and previous flux linkages respectively, and h is the integration step size.

The power converter from Fig. 1 can produce only positive current in any phase, and this should be checked in the model in case of zero or negative voltage is applied (Fig. 3b, c, and d) if the flux linkage value becomes negative:

$$\psi_k = \begin{cases} \psi_k, \psi_k \geq 0; \\ 0, \psi_k < 0. \end{cases} \tag{4}$$

The estimated flux linkage is used to evaluate the value of the current flowing in the phase winding using the desaturated

inductance value for that particular rotor position according to (1):

$$i = \frac{\psi}{L}. \tag{5}$$

This current can be smaller or bigger than the value of the saturation current. If it is smaller, then the motor operates in linear region and no correction is needed. If it is larger, the machine is in the saturation, and the actual value of the phase current should be evaluated by:

$$i = I_{sat} + \frac{\psi - L \cdot I_{sat}}{L_{min}} \tag{6}$$

instead of (5), where I_{sat} is the saturation current, and L_{min} is the minimum inductance of the winding. If the flowing current is less than saturation current value, then the torque equation of a single phase is:

$$T = \frac{1}{2} i^2 \frac{\mathrm{d}L(\theta)}{\mathrm{d}\theta} = \frac{1}{2} i^2 \frac{\mathrm{d}(L_{av} - \Delta L \cos\theta)}{\mathrm{d}\theta} = \frac{1}{2} \Delta L i^2 \sin\theta. \tag{7}$$

Evaluation of the torque above saturation current can be done with a help of co-energy, which can be defined as follows:

$$\begin{aligned} \mathrm{W}'(i,\theta) = (L_{av} - \Delta L \cos\theta)\left(\frac{I_{sat}^2}{2} + I_{sat}(i - I_{sat})\right) + \\ + L_{min} I_{sat}(i - I_{sat}), \end{aligned} \tag{8}$$

Torque can be evaluated as:

$$T = \left.\frac{\partial \mathrm{W}'(i,\theta)}{\partial\theta}\right|_i = \left(I_{sat} i - \frac{I_{sat}^2}{2}\right)\Delta L \sin\theta. \tag{9}$$

B. Losses model in the power converter

Power losses in power converters can be split between conductive and switching. Conduction losses for transistor (10) and diode (11) are obtained by multiplying the current by the voltage drop, which is obtained from a look-up table provided in the transistor data sheet [13]:

$$\Delta P_{Q\,cond} = i \cdot \mathrm{v_{CE}}(i,\tau), \tag{10}$$

$$\Delta P_{D\,cond} = i \cdot \mathrm{v_F}(i,\tau), \tag{11}$$

where $\mathrm{v_{CE}}$ is the collector to emitter voltage drop as a function of flowing current i and temperature τ; $\mathrm{v_F}$ is the diode forward characteristics.

Each commutation performed by control system results in switching losses occurring in transistor and/or reverse recovery losses in the freewheeling diode. According to [13] these losses are represented in joules. Each time the commutation occurs during the integration step these losses are converted into watts by:

$$\Delta P_{Q\,on} = E_{on}/h, \tag{12}$$

$$\Delta P_{Q\,off} = E_{off}/h, \tag{13}$$

$$\Delta P_{D\,rr} = E_{rr}/h, \tag{14}$$

where E_{on}, E_{off}, and E_{rr} are turn on, turn off and reverse recovery energies; $\Delta P_{Q\,on}$, $\Delta P_{Q\,off}$, and $\Delta P_{D\,rr}$ are turn on, turn off, and reverse recovery loss powers; and h is the integration step size.

C. Thermal model of the forced air-cooled heatsink

The heatsink and the modules configuration is depicted in Fig. 4. Power module A+ of the phase A, which feeds the motor phase with the positive voltage, is followed by the module C–, which feeds phase C with negative voltage. Then there are B+, B–, C+, and A– modules. That configuration provides equal average temperature of the power modules of each phase assuming that the losses in each phase are equal. By choosing the current path in the state with zero voltage applied from Fig. 3a or Fig. 3b, it is possible to redistribute the losses between the modules of the top side chopper and bottom side chopper.

The thermal model of the power converter obtains losses ΔP_n from six power modules located at the top of the heatsink. The heatsink itself is split into six parts having some thermal capacitance C_n (see Fig. 5). Each of these six parts is connected with adjacent parts through some thermal resistance R_{m-m} (module to module) and heat is extracted through R_{m-a} (module to ambient). The cooling air temperature varies as it passes along the ribs of the heatsink. Assuming that the airflow is constant, the air increases its temperature at each segment of the heatsink with respect to the difference between temperature of this part τ_n and the incoming air temperature $\tau_{air\,n}$ multiplied by k_τ, which depends on the airflow rate and thermal capacitance of the air.

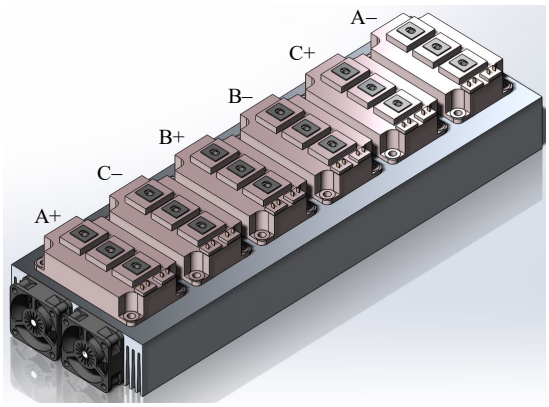

Fig. 4. Suggested configuration of the power converter for SRD.

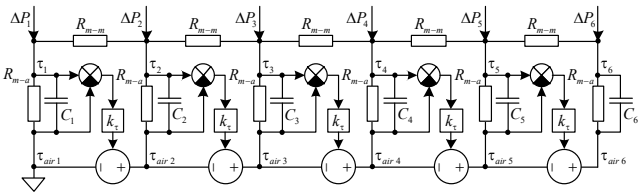

Fig. 5. Thermal model of the forced air-cooled heatsink.

III. The Model Predictive Control System

The model predictive control considers each of the possible inverter states using the considered model and then chooses one of them according to the cost function. For each phase there are four inverter states shown in Fig. 3; zero voltage states are equal in terms of control, while different in terms of losses in the power converter.

Usually, in case of conventional control strategy, the operation cycle of the phase starts from application of the DC bus bar voltage to the motor. Phase current growth is limited by the current controller which applies zero voltage or even negative voltage. The negative voltage can be applied by switching all phase switches off, while the phase current is flowing through the freewheeling diodes. Selection of the zero voltage state can be done according to the power modules temperatures. So, each phase has three distinguished states (0—all switches are off; 1—one of the switches is on; 2—both switches of the phase are on), and there are three phases in total, which gives 27 possible combinations. For each combination of the inverter state, currents, torque, and losses should be estimated as well as other parameters of the motor needed for the model operation. The model is assumed to be correct because the design of proper model lies out of the scope of the paper. These estimations are used to evaluate the cost function.

The model predictive control strategy uses a cost function, which can consider several objectives simultaneously. The primary control variable is the torque. Next, the ohmic loss minimization can be considered, maximum current limitation, and the switching loss minimization in the power converter including active thermal control, which redistributes switching losses between the power modules of each phase with respect to their current temperatures. First four objectives are resolved by:

$$g = g_1 + g_2 + g_3 + g_4, \tag{15}$$

where

$$\left.\begin{aligned} g_1 &= A\left(T_{ref}\left(1 + k_{cur}\sum_{j=a}^{c} i_j^2\right) - T\right)^2; \\ g_2 &= B\left(\sum_{j=a}^{c} i_j^2\right); \\ g_3 &= \infty \cdot \sum_{j=a}^{c}\left(I_{max} < i_j\right); \\ g_4 &= C\left(\sum_{j=a}^{c} i_j \left| s_j[k-1] - s_j[k] \right|\right), \end{aligned}\right\} \tag{16}$$

where A, B, and C are the coefficients of the cost function, T_{ref} and T are the commanded and actual torque, k_{cur} is the torque command correction coefficient, and s is the phase switches state from 0 to 2.

The first part of the cost function equation g_1 compares commanded and referenced torques. The torque reference is corrected before the compare taking into account the penalization produced by the second component of the cost function. Second component g_2 is needed to keep the ohmic losses at the minimum value. For example, if this component is absent, then the same torque can be produced by different combinations of stator current, while only one of them has minimal ohmic losses. The third component g_3 limits the phase current at the maximum permitted level. And the final component is used to penalize switching of the power converter. As the switching losses can be assumed to be proportional to the current to be switched, this part of the cost function g_4 compares the previous and new states of the power converter with respect to the flowing current of the corresponding phase.

The power modules temperature is considered twice. First, is the transient between the 2nd and 1st converter states in the drive mode. If the temperature of the top-side chopper is higher than the transient from 2nd to 1st states should be done switching bottom-side chopper (see Fig. 3b) and the switching losses occur in the power module of the bottom-side chopper. Otherwise, the top-side chopper should be switched in order to move to the state depicted in Fig. 3c. In generator mode there is a possible transient from the 1st to a zero state. If the top-side chopper has higher temperature, then the state from Fig. 3c should be chosen, and vice versa.

IV. Simulation Results

The simulation was performed with a sampling frequency 120 kHz, as well as the simulated control system. The parameters of drive are listed in TABLE I. The thermal capacitance of the heatsink was reduced in order to speed up the transients and decrease the simulation time.

TABLE I. SRD Parameters Including Heatsink

Parameter	***Value***	***Units***
Minimal inductance	1.0	mH
Maximum inductance	10.0	mH
Saturation current	20	A
Phase resistance	0.05	Ohm
Pole pairs	4	-
Maximum phase current limit	100	A
DC link voltage	600	V
Thermal capacitance heatsink segment	0.1	$\frac{\text{J}}{\text{kg}\times\text{K}}$
Thermal resistance between heatsink segments	2.0	K/W
Thermal resistance from heatsink segment to ambient	1.34	K/W
k_τ	0.054	-

The operation of the fully tuned cost function is shown in Fig. 6, when $A = 1$, $B = 0.0005$, $C = 0.0015$, and $k_{cur} = 0.00002$. The torque has reached the referenced value, and the heatsink segments temperatures have grown simultaneously.

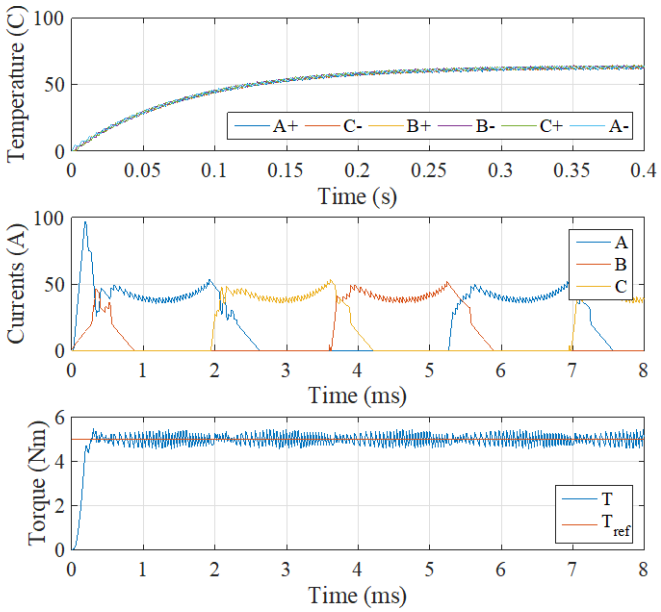

Fig. 6. Operation of the model predictive control system with fully tuned cost function. From top to bottom: temperatures of each power module, phase currents, referenced and actual torques.

The *B* coefficient helps to keep the ohmic losses at the minimum possible level. If it is equal to zero together with k_{cur}, then the current shape changing as it is shown in Fig. 7. Moreover, the phase current stays at the high level even if it is possible to obtain the same torque with the smaller current of another phase. Then the torque of the phase becomes too small due to decrease of the inductance derivative, but it takes time to increase the current of another phase to keep the commanded torque. This results in the torque pulsations during phase change.

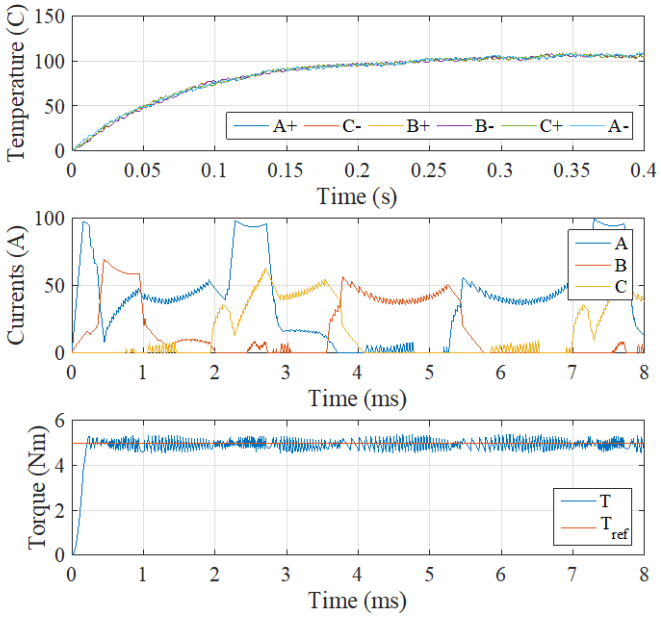

Fig. 7. Operation of the model predictive control system without considering ohmic losses component in the cost function (coefficients *B* and k_{cur} are equal to zero). From top to bottom: temperatures of each power module, phase currents, referenced and actual torques.

When the first and second parts of the cost function compete, the k_{cur} coefficient helps to add some value proportional to the flowing current to torque reference in order to keep the actual torque near the commanded value. If k_{cur} is equal to zero, then the control system implements the torque reference with some error as shown in Fig. 8.

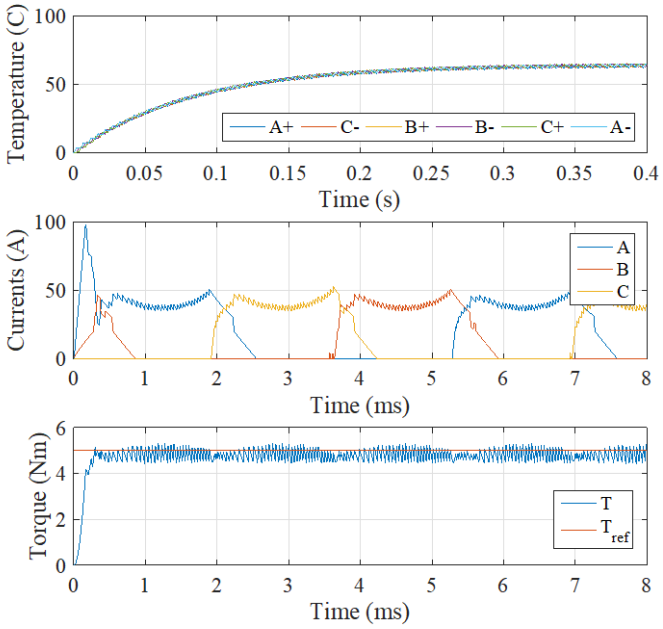

Fig. 8. Operation of the model predictive control system without referenced torque correction in the cost function (coefficient k_{cur} is equal to zero). From top to bottom: temperatures of each power module, phase currents, referenced and actual torques.

By making the *C* coefficient equal to zero, the torque command is tracked more precisely, while the switching rate increased together with the losses and the temperature of the power modules as shown in Fig. 9.

At last, the switching off active thermal control with heat dissipation balancing leads to increase of the difference between power module temperatures as shown in Fig. 10. The temperature of the hottest IGBT module increased from 88.4°C to 95.0°C. This example shows that proper placement of the IGBT modules and dissipation balancing algorithm would allow an increase in the output power of the power electronics converter around 7% for this particular case.

V. Conclusions

The problem of precise torque control of a switched reluctance drive, which is known by its torque pulsations, was considered in this paper. It is suggested to improve drive performance by means of control algorithms. The proposed control strategy using model predictive control provides efficient and precise torque control for a switched reluctance machine. The cost function can consider several parameters which can be adjusted in order to achieve desired operation mode. Active thermal control allows heat dissipation balancing and eventually to increase the output power of the electronic converter. Still the control strategy needs the model of the

electrical machine, whose accuracy strongly affects the performance in the produced torque.

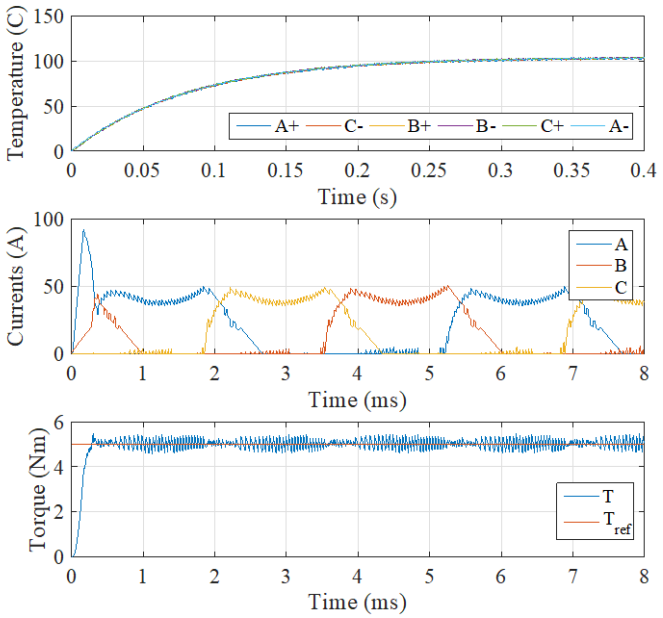

Fig. 9. Operation of the model predictive control system without switching rate control in the cost function (coefficient *C* is equal to zero). From top to bottom: temperatures of each power module, phase currents, referenced and actual torques.

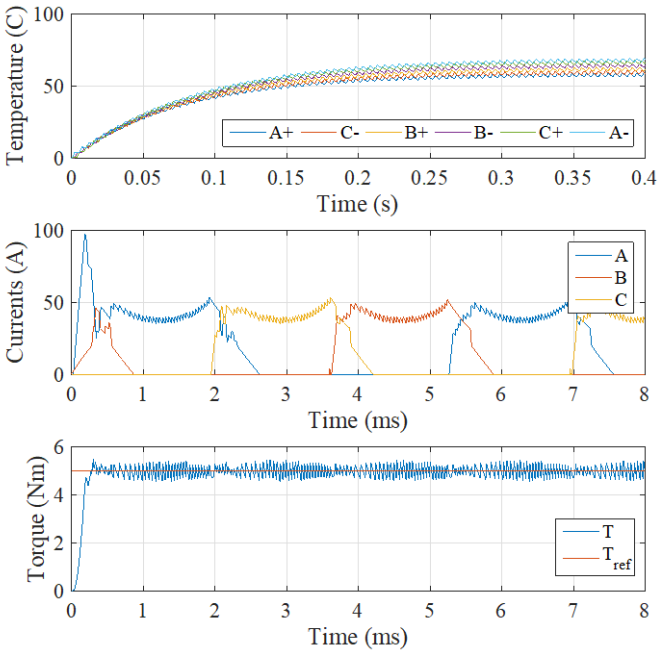

Fig. 10. Operation of the model predictive control system without active thermal control. From top to bottom: temperatures of each module, phase currents, referenced and actual torques.

REFERENCES

[1] R. Krishnan, Switched reluctance motor drives: modeling simulation analysis design and applications, CRC Press, 2001.

[2] N. A. Patil, J. S. Lawler, "Issues in the control of the switched reluctance motor during continuous conduction," in proc. of 2007 39th North American Power Symposium, 2007, pp. 534–540, doi: 10.1109/NAPS.2007.4402362.

[3] M. Rekik, M. Besbes, C. Marchand, B. Multon, S. Loudot, D. Lhotellier, "Improvement in the field-weakening performance of switched reluctance machine with continuous mode," IET Electric Power Applications, vol. 1, no. 5, pp. 785–792, doi: 10.1049/iet-epa:20070069.

[4] A. Anuchin, M. Lashkevich, D. Aliamkin, F. Briz, "Achieving maximum torque for switched reluctance motor drive over its entire speed range," 2017 International Symposium on Power Electronics (Ee), pp. 1-6, 2017.

[5] Iqbal Husain, "Minimization of Torque Ripple in SRM Drives," IEEE Trans. Industrial Electronics, vol. 49, no. 1, Feb. 2002.

[6] L. Venkatesha, V. Ramanarayanan, "Torque Ripple Minimisation in Switched Reluctance Motor with Optimal Control of Phase Currents," Proceedings of the 1998 IEEE International conference on Power Electronics Drives and Energy Systems, vol. 2, pp. 529-534, 1998.

[7] S. Pratapgiri, "Comparative Analysis of Hysteresis Current Control and Direct Instantaneous Torque Control of Switched Reluctance Motor," International Conference on Electrical Electronics and Optimization Techniques (ICEEOT), 2016.

[8] J. Jing, S. Lv, C. f. Shi, "Direct torque PID control of switched reluctance motor based on duty ratio control technique," 2015 IEEE International Conference on Mechatronics and Automation (ICMA), pp. 649-653, 2015.

[9] R. B. Inderka R. W. A. A. De Doncker "DITC-direct instantaneous torque control of switched reluctance drives," Industry Applications IEEE Transactions on vol. 39, pp. 1046-1051, 2003.

[10] I. Castro, P. Andrada, B. Blanque, "Minimization of torque ripple in switched reluctance motor drives using direct instantaneous torque control," in Proc. ICEM2012, pp. 1021-1026, Sept. 2012.

[11] H. Peyrl G. Papafotiou and M. Morari "Model predictive torque control of a switched reluctance motor," in Industrial Technology 2009, ICIT 2009, IEEE International Conference on, pp. 1-6, Feb. 2009.

[12] A. Anuchin, D. Savkin, Y. Khanova, D. Grishchuk, "Real-time model for motor control coursework," Proc. IEEE 5th Int. Conf. on Power Engineering Energy and Electrical Drives POWERENG, pp. 427-430, 11–13 May 2015.

[13] Fast IGBT4 Modules, SKM100GAL12T4, Semikron, Rev. 1 – 03.09.2013